Direct Observation of Diffuse Cone Behavior in de Vries Smectic-*A* and -*C* Phases of Organosiloxane Mesogens

HyungGuen Yoon,[1] Dena M. Agra-Kooijman,[1] Khurshid Ayub,[2] Robert P. Lemieux,[3] and Satyendra Kumar[1]
[1] *Department of Physics, Kent State University, Kent, Ohio 44242, USA*
[2] *Department of Chemistry, COMSATS Institute of Information Technology, Abbottabad, 22060, Pakistan*
[3] *Department of Chemistry, Queen's University, Kingston, Ontario, Canada K7L 3N6*

(Received 16 November 2010; published 24 February 2011)

Simultaneous and direct x-ray measurements of the smectic layer spacing, molecular tilt, and orientational order in the de Vries smectic *A* (Sm*A*) and *C* (Sm*C*) phases of two organosiloxane mesogens reveal that (i) the Sm*C* (tilt) order parameter exponent $\beta = 0.26 \pm 0.01$ for 2nd order Sm*A*-Sm*C* transition—in excellent agreement with the tricritical behavior, (ii) the siloxane and hydrocarbon parts of the molecules are segregated and oriented parallel to the director with very different degree of orientational order, and (iii) thermal evolution of the effective molecular length is different in the two phases.

DOI: 10.1103/PhysRevLett.106.087801 PACS numbers: 61.30.Gd, 61.30.Eb, 64.70.mj

In the smectic *A* (Sm*A*) and smectic *C* (Sm*C*) liquid crystal (LC) phases, calamitic molecules are arranged in layers with no positional order in directions parallel to the layers. These phases possess a relatively high degree of molecular orientational order $S = \langle 3\cos^2\theta - 1\rangle/2$, where θ is the angle molecules on average make with the common direction $\boldsymbol{n}$, referred to as the *director*. In the uniaxial Sm*A* phase, $\boldsymbol{n}$ is parallel to the layer normal, i.e., the z direction as shown in Fig. 1. However, $\boldsymbol{n}$ develops a (polar) tilt angle $\alpha(T)$ relative to z at the transition to the Sm*C* phase at the temperature T_{AC}. Below T_{AC}, the value of smectic layer spacing, d, decreases by a factor of $\cos[\alpha(T - T_{AC})]$ as $\alpha(T)$ increases [1]. In most cases, the director simply develops a polar tilt in a specific azimuthal direction. Maximum layer-shrinkage in a typical Sm*C* phase can [1,2] be as high as ~11%.

In 1979, de Vries, *et al.* [3–5], reported quantitatively very different behavior at the Sm*A*-Sm*C* transition of *trans*-1,4-cyclohexane-*di*-*n*-octyloxy-benzoate (TCOOB). They found d in the Sm*A* phase to be significantly smaller than the molecular length, L, and the layer-shrinkage in the Sm*C* phase of less than 1%. These are now known as the *de Vries's smectic phases*. They proposed an elegant *diffuse-cone model* [3–6] to explain the unusual properties of these materials. According to the model, molecules in the Sm*A* phase on average are oriented at a large polar angle with respect to z, but their orientation is azimuthally degenerate; see Fig. 1. The local director is uniformly distributed on the surface of a cone with its axis parallel to z. Azimuthal degeneracy is lost at T_{AC}. In the Sm*C* phase, the distribution gradually becomes narrow and biased towards a specific azimuthal direction generating an effective director tilt without a significant change in the molecular polar tilt and only a minimal layer shrinkage. Their small layer-shrinkage offers a pathway to eliminate chevron defects [7] in ferroelectric SmC^* based displays. In these devices, large layer shrinkage causes chevron defects and bright zigzag lines, which have hindered their commercialization for decades. Consequently, a large number of de Vries smectic mesogens have been synthesized [8–11] in recent years. Generally, these mesogens have either a perfluorinated or a siloxane segment in one of the end-chains that tends to nanosegregate and enhance lamellar order, which is believed to promote the de Vries behavior [12–14].

The conventional Sm*A*-Sm*C* transition is normally second order and is described by its order parameter; $\alpha(T) = \alpha_o(T_{AC} - T)^\beta$. For these materials, it was possible to determine $\alpha(T)$ from the splitting of the small-angle x-ray diffraction peaks and from changes in the values of d, and acquire a large number of data points close to the transition [15]. The nature of this phase transition was characterized and modeled [15–17] some time ago providing a somewhat complete picture. However, in the de Vries smectic phases, this transition is often found to be first order. There appears to be a consensus that the continuous Sm*A*-Sm*C* transitions in de Vries materials occur in the proximity of a tricritical point [18,19]. Systematic increase in molecular size [11,20] changes the transition from second to first order with increasing enthalpy of transition.

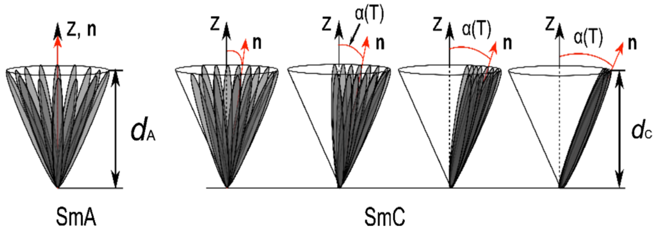

FIG. 1 (color online). Diffuse-cone model: polar tilt of molecules remains relatively unchanged while the uniform azimuthal distribution of the Sm*A* phase gradually loses its degeneracy in the Sm*C* phase increasing the effective tilt angle at lower temperatures.

Generalized Landau [18] and molecular statistical [19] theories provided important insights into the nature of these systems. While most of the experimental results can be explained within the framework of the *diffuse-cone* model, the results reported in this Letter provide the first direct structural evidence of the diffuse-cone behavior that has so far been lacking.

Using the wealth of knowledge on de Vries materials acquired in the past decade, Roberts, *et al.*, [20] have recently synthesized a homologous series, Fig. 2, with a trisiloxane-terminated undecyloxy chain, a 5-phenylpyrimidine core, and an alkyloxy end chain. Enthalpy of the Sm*A*-Sm*C* transition is immeasurably small for molecules with 4–6 carbon end-chains, increasing gradually to ~1.7 kJ/mol for the 9th homolog (C9). We have performed synchrotron x-ray study of the C4 and C9 compounds exhibiting second and first order Sm*A*-Sm*C* transitions, respectively.

The samples were filled in 2 mm diameter quartz Lindéman capillaries, flame-sealed, and placed inside an Instec (HCS402) hotstage with a precision of ±0.1 °C. Samples were heated to a temperature well above the clearing point in the presence of an *in situ* magnetic field of ~2.5 kG. Even without a nematic phase, we were able to obtain monodomain samples by repeatedly heating and cooling across the clearing point while monitoring the quality of alignment via x-ray diffraction. The weak magnetic field was mostly inconsequential in smectic phases.

X-ray measurements were made at the undulator beamline station 6IDB of the Midwestern Universities Collaborative Access Team's (MuCAT) sector at the Advanced Photon Source using 16.2 keV ($\lambda = 0.76534$ Å) photons. A pair of X-Y slits was used to define the incident x-ray beam cross section to 100 μm × 100 μm. An image plate detector MAR345 was placed at a distance of 506.4 mm (for C4) and 517.4 mm (for C9) from the sample. The incident flux was sufficiently attenuated to avoid sample radiation damage. A silicon standard (NIST 640C) was used to calibrate the spectrometer. Background scattering was recorded using an empty capillary and subtracted from the data. The 2θ–θ and χ scans were generated from 2D diffraction patterns using the FIT2D software package [21]. These scans were used to calculate structure parameters and to estimate S using the method of Davidson, *et al.*, [22].

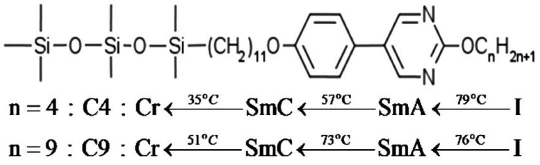

FIG. 2. Molecular structures and phase sequence of C4 and C9 compounds. Here, I and Cr are abbreviations for the isotropic and crystal phases, respectively.

Representative wide-angle diffraction patterns in the Sm*A* (57.2 °C) and Sm*C* (55.7 °C) phases of C4, shown in Fig. 3, reveal at least three harmonics of the small-angle peak (joined by short dotted lines) corresponding to the smectic layer spacing. Four harmonics are observed in the Sm*C* phase of C9. These establish that the smectic order parameter is high and smectic density wave is strongly condensed.

In the direction perpendicular to small-angle peaks, there are two pairs of arclike reflections (green and green with orange central part) corresponding to lateral separation between the hydrocarbon (of 4.5 Å) and siloxane (~ 6.8 Å) parts of the molecule. The centers of these reflections fall on the long solid line suggesting that the siloxane and the hydrocarbon parts both are oriented parallel to ***n*** in both phases. This constitutes the only

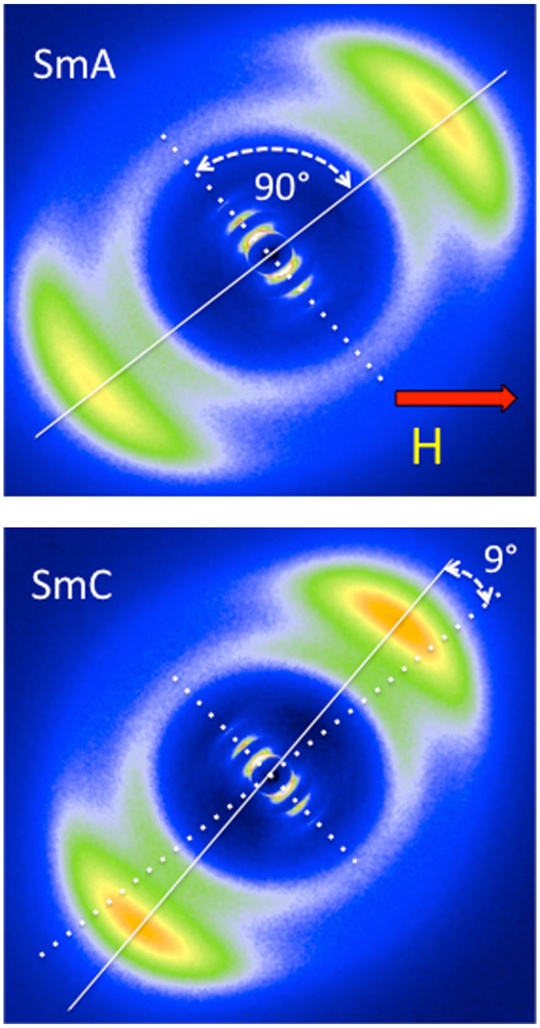

FIG. 3 (color online). Representative diffraction patterns in the Sm*A* phase at 57.2 °C and the Sm*C* phase at 55.7 °C, of mesogen C4 illustrating a change in molecular tilt from 0° in the Sm*A* phase to 9° in the Sm*C* phase. The dotted line passing through the large angles peaks of the Sm*C* phase represents their orientation in the Sm*A* phase.

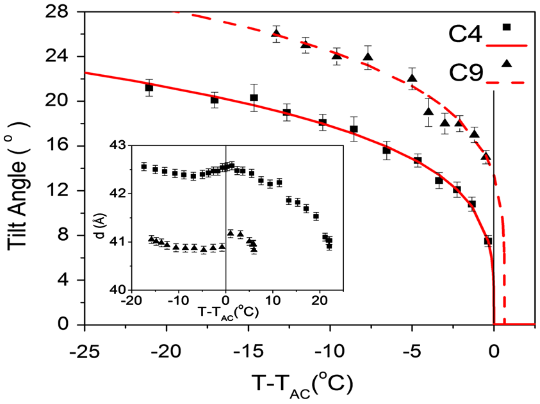

FIG. 4 (color online). Temperature dependence of tilt angle for the two compounds. Line (red) graphs represent fits with order parameter exponent $\beta = 0.26 \pm 0.01$ for the second order Sm*A*-Sm*C* transition of C4 and $\beta = 0.21 \pm 0.02$ at the first order transition of C9. The inset shows temperature dependence of d for C4 and C9.

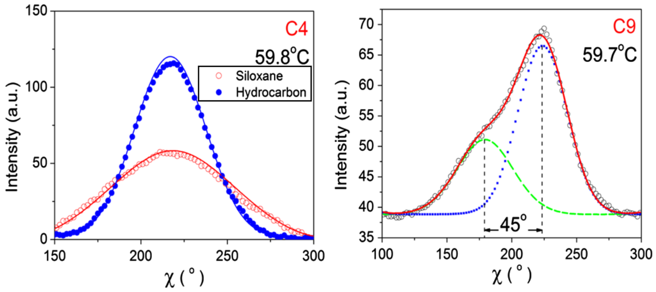

FIG. 5 (color online). Left: χ scans through the two large angle peaks arising from lateral separation between siloxane and hydrocarbon sections of the C4 molecule in the Sm*A* phase. Right: χ scans through the hydrocarbon peak in the Sm*C* phase (59.7 °C) of C9. Solid line represents the fit to calculate S for the two domains misoriented by ~45° with respect to each other. Fits to the two domains are represented by the dashed (green) and dotted (blue) plots.

known direct evidence of previously inferred [12–14] nanosegregation of siloxane segments. The two (dotted and solid) lines drawn over the small and large angle peaks in Figs. 3 are at 90° to each other in the Sm*A*, i.e., $\alpha(T) = 0°$. In the Sm*C* phase, they become oblique as $\boldsymbol{n}$ tilts away from the z-direction by an angle $\alpha(T)$, which can be quantitatively and directly obtained from the χ-scans. In the case of C4, $\alpha(T)$ is 9° at 55.7 °C, i.e., 1.5 °C below T_{AC}.

Temperature dependences of the order parameter $\alpha(T)$ for C4 and C9 are plotted in Fig. 4 along with simple power law fits. The order parameter critical exponent β is 0.26 ± 0.01 and 0.21 ± 0.02 for compounds C4 and C9, respectively. The transition temperature obtained from the fit to C4 data is, within experimental uncertainties, indistinguishable from the actual transition temperature, T_{AC}. The value of β for C4 is in excellent agreement with the theoretical expectation of tricritical behavior. In the case of C9, we observe a large jump in $\alpha(T)$, a finite enthalpy of transition [20], and a difference of ~0.7 °C between the virtual (fitted) second order transition temperature and T_{AC}. A smaller value of β ($= 0.21$) is also understandable at this first order transition.

Owing to good alignment of our samples, it was possible to generate separate χ-scans for the fully resolved siloxane and hydrocarbon peaks; see Fig. 5. The siloxane peaks are clearly wider than the hydrocarbon peaks, suggesting a lower value of S for the former. Temperature dependence of S [22] for both parts of the molecule are shown in Fig. 6. Sample C4 remained a monodomain and the value of S in the Sm*A* phase was close to 0.7. In the Sm*C* phase, it slowly increases to a plateau at 0.78. The value of S for the siloxane segments is ~0.45, shows no significant change across the transition, and gradually diminishes to ~0.41 in the Sm*C* phase. Since the siloxane segment is linked by an 11-carbon chain to the rigid core, it should have significant orientational freedom and thus, a smaller S.

These values of S are higher than previously reported [20] in de Vries mesogens and comparable to a typical nematic. However, it is important to note that previously reported values are for entire molecule and not for its two different segments. Furthermore, since de Vries materials do not form a nematic phase, it is very hard to obtain well-aligned single domains using normally accessible external fields. Clearly, if the sample is poorly aligned and/or a broad x-ray beam which illuminates a large number of misaligned domains is used, the measured S will invariably be smaller than the actual value. This may have been a factor responsible for lower estimates of S in previous studies. We were able to align samples well by repeatedly heating and cooling and the small x-ray beam cross section ($100 \times 100\ \mu\mathrm{m}^2$) allowed us to probe single domains. Nevertheless, the alignment of smectic phases in our experiments may not be perfect, and the S values reported here should be taken as lower limits.

Sample of C9 started out as a single domain in the Sm*A* phase but split into two domains upon entering the Sm*C*

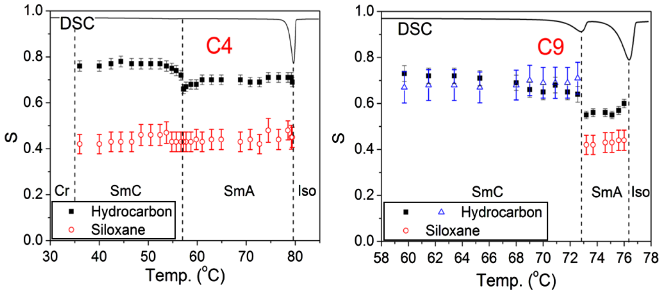

FIG. 6 (color online). Temperature dependence of the orientational order parameter S for C4 and C9 calculated for the hydrocarbon and siloxane peaks at 4.5 and 6.8 Å, respectively. DSC results on top are taken from Ref. [20].

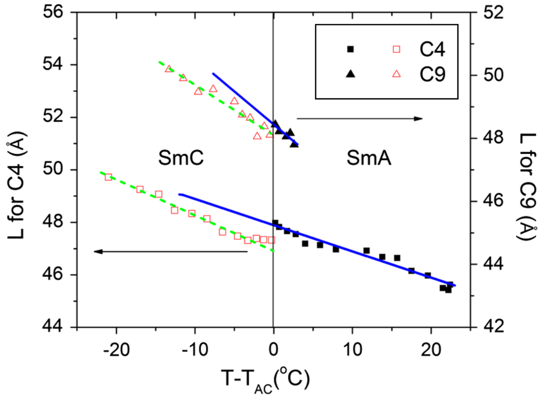

FIG. 7 (color online). Temperature dependence of the effective molecular length L in the SmA and SmC phases of C4 and C9. Solid and dashed lies are linear fits to the data.

phase as evident from the asymmetric structure of the large angle hydrocarbon x-ray peak, Fig. 5. The two domains were misaligned by ~45° relative to each other. The composite SmC peak was analyzed using a sum of two S functions (shown in Fig. 5) centered at different values of χ to fit the data. Same values of S were obtained from the two domains, which increase from 0.62 to 0.75. The values of S in the SmA phase for the hydrocarbon and siloxane segments are ~0.55 and 0.40, respectively. A jump of $\Delta S = 0.1$ is observed at this first order transition consistent with DSC results from reference [20] plotted at the top in Fig. 6. In the SmC phase of C9, the siloxane peak became too weak to allow a reliable estimate of S.

Temperature dependence of d shown in the inset of Fig. 4 reveals that *maximum layer shrinkage* does not exceed 0.4% and 0.9% for in the SmC phase of C4 and C9, respectively. The *effective* molecular length, $L(T)$, Fig. 7, calculated using the equation [23], $L(T) = 3d/[(S+2)\cos\alpha(T)]$ and our directly and independently measured values of d and $\alpha(T)$. An important finding is that the temperature dependence of L is different in the two phases. Until now, L has been assumed [20,23] to either remain constant in the SmC phase at the highest value of d measured at the SmA-SmC transition, or change [5] linearly with temperature at the same rate as in the SmA phase. This result should help researchers reexamine previously made assumptions in data analysis and modeling, and better understanding the de Vries materials.

To summarize, we have for the first time *directly* accessed the director tilt, orientational order parameters of both the hydrocarbon and siloxane parts of the molecule, and calculated the effective molecular length in both phases. The results reveal up to four multiples of the smectic Bragg peak confirming highly developed smectic order in both phases. Large angle peaks arising from the hydrocarbon and siloxane segments of the molecules are separable and allow calculations of thermal evolution of the corresponding orientational order parameters. The values of S are found to be higher than previously reported in similar and different de Vries compounds but smaller than in conventional SmA and SmC phases. Temperature dependence of S for the nanosegregated siloxane segments residing at the smectic layer interface is also determined. The SmC order parameter exponent β calculated from directly measured tilt angle is 0.26 ± 0.01 for C4 in excellent agreement with tricritical and 2D Ising behavior.

The authors are grateful to P. Collings, D. Allender, N. Clark, and F. Giesselmann for helpful discussions. This work was supported by the US Department of Energy (DOE), Basic Energy Sciences grant (BES) ER46572 and by the Natural Sciences and Engineering Research Council of Canada. The use of the Advanced Photon Source was supported by the US DOE, BES, under Contract No. W-31-109-Eng-38. MuCAT's sector at the APS is supported by the US DOE, BES, through the Ames Laboratory under Contract No. W-7405-Eng-82.

[1] S. Kumar, Phys. Rev. A **23**, 3207 (1981).
[2] J. P. Lagerwall and F. Giesselmann, Chem. Phys. Chem. **7**, 20 (2006).
[3] A. deVries, A. Ekachai, and N. Spielberg, Mol. Cryst. Liq. Cryst. **49**, 143 (1979).
[4] A. de Vries, J. Chem. Phys. **71**, 25 (1979).
[5] A. deVries, A. Ekachai, and N. Spielberg, J. Phys. (Paris) **40**, C3-147 (1979).
[6] A. J. Leadbetter and E. K. Norris, Mol. Phys. **38**, 669 (1979).
[7] T. P. Rieker *et al.*, Phys. Rev. Lett. **59**, 2658 (1987).
[8] M. D. Radcliffe *et al.*, Liq. Cryst. **26**, 789 (1999).
[9] J. Naciri, C. Carboni, and A. K. George, Liq. Cryst. **30**, 219 (2003).
[10] L. Li *et al.*, J. Mater. Chem. **17**, 2313 (2007).
[11] K. Goossens *et al.*, Langmuir **25**, 5881 (2009).
[12] P. J. Collings, B. R. Ratna, and R. Shashidhar, Phys. Rev. E **67**, 021705 (2003).
[13] T. Murias *et al.*, Liq. Cryst. **29**, 627 (2002).
[14] Y. Takanishi *et al.*, Mol. Cryst. Liq. Cryst. **199**, 111 (1991).
[15] R. J. Birgeneau *et al.*, Phys. Rev. A **27**, 1251 (1983); C. R. Safinya *et al.*, Phys. Rev. B **21**, 4149 (1980).
[16] S. Dumrongrattana *et al.*, Phys. Rev. A **34**, 5010 (1986).
[17] M. A. Anisimov *et al.*, J. Phys. (Paris) **46**, 2137 (1985).
[18] K. Saunders *et al.*, Phys. Rev. Lett. **98**, 197801 (2007); K. Saunders, Phys. Rev. E **80**, 011703 (2009); K. Saunders, Phys. Rev. E **77**, 061708 (2008).
[19] M. V. Gorkunov *et al.*, Phys. Rev. E **75**, 060701 (2007).
[20] J. C. Roberts *et al.*, J. Am. Chem. Soc. **132**, 364 (2010).
[21] A. P. Hammersley *et al.*, High Press. Res. **14**, 235 (1996).
[22] P. Davidson, D. Petermann, and A. M. Levelut, J. Phys. II (France) **5**, 113 (1995).
[23] J. P. F. Lagerwall, F. Giesselmann, and M. D. Radcliffe, Phys. Rev. E **66**, 031703 (2002).